Dislocation generation mechanisms in heavily boron-doped diamond epilayers

D. Araujo, F. Lloret, G. Alba, M. P. Alegre, and M. P. Villar

COLLECTIONS

Paper published as part of the special topic on Ultrawide Bandgap Semiconductors

View Online   Export Citation   CrossMark

Dislocation generation mechanisms in heavily boron-doped diamond epilayers

View Online   Export Citation   CrossMark

D. Araujo,[1,a)] F. Lloret,[2] G. Alba,[1] M. P. Alegre,[1] and M. P. Villar[1]

AFFILIATIONS

[1]Dpt. Ciencia de los Materiales e IM y QI, Universidad de Cádiz, 11510 Puerto Real, Spain
[2]Dpt. Física Aplicada, Universidad de Cádiz, 11510 Puerto Real, Spain

Note: This paper is part of the Special Topic on Ultrawide Bandgap Semiconductors.
[a)]Author to whom correspondence should be addressed: daniel.araujo@uca.es

ABSTRACT

Doping diamond layers for electronic applications has become straightforward during the last two decades. However, dislocation generation in diamond during the microwave plasma enhanced chemical vapor deposition growth process is still not fully understood. This is a truly relevant topic to avoid for an optimal performance of any device, but, usually, it is not considered when designing diamond structures for electronic devices. The incorporation of a dopant, here boron, into a lattice as close as that of diamond, can promote the appearance of dislocations in the epilayer. The present contribution analyzes the different processes that can take place in this epilayer and gives some rules to avoid the formation of dislocations, based on the comparison of the different dislocation generation mechanisms. Indeed, competitive mechanisms, such as doping atom proximity effect and lattice strain relaxation, are here quantified for heavily boron-doped diamond epilayers. The resulting growth condition windows for defect-free heavily doped diamond are here deduced, introducing the diamond parameters and its lattice expansion in several previously published critical thickness (h_c) and critical doping level relationships for different doping levels and growth conditions. Experimental evidence supports the previously discussed thickness-doping-growth condition relationships. Layers with and without dislocations reveal that not only the thickness but also other key factors such as growth orientation and growth parameters are important, as dislocations are shown to be generated in epilayers with a thickness below the People and Bean critical thickness.

The outstanding properties of diamond, in terms of radiation resistance, breakdown electric field, carrier mobility, and thermal conductivity, make it an ultimate semiconductor for electronic device manufacture applied to high radiation environments and high power and/or high frequency applications.[1–3] The device structure, for either diodes or transistors, requires the incorporation of dopants into the diamond lattice to get their highest performances. However, the design of the device is usually focused in terms of bandgap variations and electrical field distribution in it, while criteria for the defect generation associated with the doping level are not generally considered.

Defects, especially extended defects such as dislocations, are an important issue associated with the right performance of electronic devices, even more than point defects.[4,5] Some authors[5] have described them as a function of their effect on the performance of the devices, so that they distinguish between "killer" and "non-killer" defects, with killer defects causing fatal malfunctioning in the electronic device

fabricated on the CVD film and non-killer defects causing no malfunctioning. HPHT substrates used to grow CVD diamond layers always contain defects, which are inherent to the synthesis process. Although the best substrates are chosen to grow the full structure of the device, such defects are impossible to avoid and threading dislocations (TDs) are reported in the literature on CVD boron-doped diamond layers.[6,7] Besides, the approach of considering the incorporation of the dopant in the diamond lattice as a generator of extended defects due to the lattice mismatch (misfit dislocations) must also be taken into account, not only the threading of those coming from the HPHT substrate. Some works on co-doping as a strategy for compensating the boron-induced strain in the diamond lattice have been reported.[8,9] In any case, it is essential to define clear rules that allow growing of CVD-doped diamond without dislocations, that is, with crystalline quality high enough to be used for electronic device manufacture.

Depending on desired n-type or p-type performance of diamond, phosphorous, and boron are the main dopants included for electronic applications. Due to the really reduced size of the diamond reticular lattice, incorporation of atoms at high doping levels is still challenging for the n-type and not straightforward for the p-type diamond. These difficulties take their origin in the lattice strain induced by the dopant atoms during substitutional site lattice incorporation. At high doping levels, epilayers are either strongly strained or contain dislocations, which can be generated in the diamond lattice with the resulting damage in the further fabricated electronic device. For other semiconducting materials, strain induced by the dopant incorporation never reaches such a level that dislocations are required to relax the lattice strain, but this occurs for epitaxial growth of alloys where their composition varies layer after layer. While in other semiconducting materials such as III–V or SiGe alloys, critical thicknesses determine when plastic relaxation starts,[10–13] in diamond, the problem is shown to be different in some case.[14,15] Indeed, the atomic size of the dopant, when deposited at the surface and during the growth process, locally generates 2D atomic displacements of the lattice in such a way that the incorporation of new atoms at the growth surface cannot take place without generating a dislocation.[14,15] This 2D effect is produced when atoms arise at the diamond surface and, thus, varies with the growth conditions and with the growth orientation, as the planar atomic density also changes. This is a local "geometrical" effect and not an energy balance mechanism as, for example, the Matthew and Blakeslee[10] or the People and Bean[11] ones. For the case of diamond doping during microwave plasma enhanced chemical vapor deposition (MPCVD) growth, several mechanisms can coexist in the same range of doping. Thus, to define growth conditions to obtain dislocation-free doped diamond, these mechanisms should be compared and quantified. This is the aim of this work, using transmission electron microscopy (TEM) dislocation observations to discuss a particular case. Conditions for growing dislocation-free diamond are then established.

Here, four different samples are used, grown by microwave plasma enhanced chemical vapor deposition (MPCVD) over HPHT diamond substrates. Sample #1 is a heavily boron-doped diamond layer grown along the $\langle 111 \rangle$ orientation, with 0.15% of CH_4/H_2, methane content, and 2×10^{21} at/cm^{-3} of boron. Sample #2 is a 111-oriented multilayered doped/undoped sample. Boron-doped layers of 20 nm were obtained using 0.5% of CH_4/H_2, with a boron concentration of 2.3×10^{21} at/cm^{-3}. Sample #3 is a multilayered δ-doped/undoped sample grown along the $\langle 111 \rangle$ direction. The CH_4/H_2 ratio, used in doped layers, was 0.25%. The boron concentration and layer thickness are 10^{19} at/cm^{-3} and 6 nm, respectively. Sample #4 is a $\langle 100 \rangle$ multilayered structure. 50 nm boron-doped layers were deposited using 0.5% of CH_4 over H_2 + He with a doping content of 2×10^{21} at/cm^{-3}. Samples were observed by TEM using a Jeol 2010F microscope at 200 keV.

The misfit between lattices of an epilayer and its substrate is accommodated either by misfit strain (elastic accommodation of the lattice through tetragonal distortion in the case of diamond) or by misfit dislocations (MD, plastic relaxation) and residual misfit strain. Indeed, some residual strain always remains after plastic relaxation, as some energy is always required to generate dislocations. For relative simplicity, the problem of strain relief due to the generation of MDs has mostly been considered at the equilibrium limit, using the equilibrium principle as approximated by minimum energy E of the system.

A dislocation will be formed only if the relieved elastic strain energy of the epilayer is larger than the energy associated with the dislocation itself. For an elastically strained epitaxial monolayer (ML), the thicker the layer is, the larger the elastic strain energy is. At a certain thickness, plastic relaxation is favored through dislocations that can adapt the in-plane lattice space of both the substrate and the epilayer. The energy associated with dislocation segments depends primarily on bonding and, thus, on the considered material. When growth continues with the formation of a multilayer, misfit dislocations follow to adapt lattices from layers above this commonly labeled critical thickness, h_c. Several criteria have been proposed to evaluate this h_c, depending mostly on the material system. In following paragraphs, the most used ones are compared for the case of boron-doped diamond layers.

In Fig. 1, the critical thicknesses above which dislocations are generated to relax the lattice strain are graphed vs the lattice mismatch between the epilayer and the substrate for the samples studied here. This mismatch, f, is defined as

$$f = \frac{a(x) - a_0}{a_0}, \qquad (1)$$
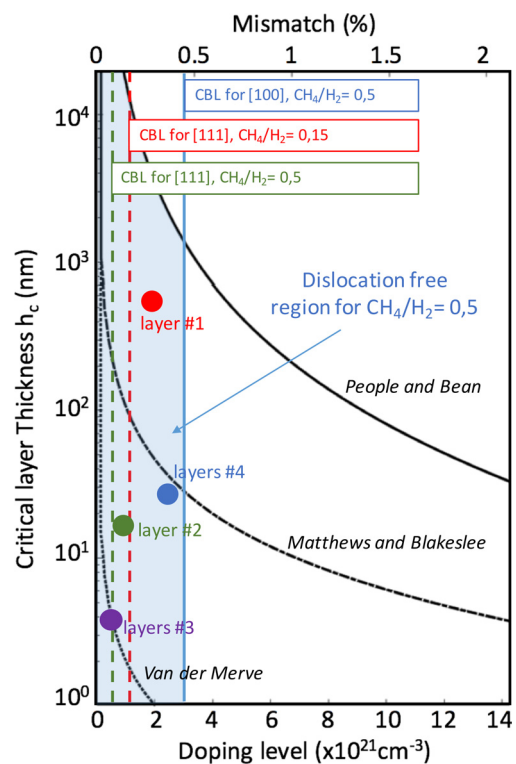
FIG. 1. Critical thickness, h_c, vs mismatch and boron doping level in diamond boron-doped epilayers grown on diamond undoped substrates. Red, green, pink, and purple colors are related to the samples studied here. The red, green, and blue lines indicate the critical boron doping level (CBL) for the CH_4/H_2 ratio and the growth orientation used in each sample (see Fig. 2; note that the CBL cannot be determined for sample #3). The blue area evidences the resulting conditions for a dislocation-free MPCVD growth for a CH_4/H_2 ratio of 0.5% growing along [100]. As shown in Fig. 2, the layers located on the right-hand side with respect to their CBL lines present dislocations.

with $a(x)$ being the epilayer lattice parameter for a certain boron dopant concentration x and a_0 the undoped diamond substrate lattice parameter. The variation of the lattice parameter with respect to the boron concentration has been previously reported and follows a linear law below 2% at. with a slight saturation above this value. Therefore, to obtain $a(x)$ in nm units, we interpolate the data in the study by Brazhkin et al.,[16] in the linear range (<2% [B]) as follows:

$$a(x) = 0.3566 + 5.3 \times 10^{-4}x. \tag{2}$$

In the present case, dislocation generation in a heavily boron-doped epilayer grown on an undoped diamond substrate is analyzed. Here, the three most referred models of lattice relaxation in the literature are chosen and compared: Matthews and Blakeslee[10] (M–B), People and Bean[11] (P–B), and Van der Merwe[12] (V-M). All of them offer an answer to the moment in which dislocations begin to "contaminate" the epilayer as a result of uniform mismatched related strain in the 2D grown epilayer. The Matthews and Blakeslee (M–B) approach[10] defines an equilibrium critical thickness above which the blowing out or bending of existing threading dislocations (TDs) occurs. This model was initially developed for the GaAs/GaAsP system, where existing threading dislocations coming out from the substrate bend to become misfit dislocations. Therefore, the critical thickness, h_c, can be determined as follows:

$$h_c \cong \left(\frac{b}{f}\right)\left[\frac{1}{4\pi(1+\nu)}\right]\left[\ln\left(\frac{h_c}{b}\right) + 1\right], \tag{3}$$

where b is the Burger vector and ν the Poisson factor. The People and Bean approach,[11] however, is different: it assumes that the misfit dislocation generation is solely determined by an energy balance. This approach differs from the M–B one, in which just mechanical equilibrium of a grown-in threading dislocation determines the onset of interfacial misfit dislocations. Instead, the P–B model proposes that the growing film is initially free of threading dislocations, so that interfacial misfit dislocations will be generated when the areal strain energy density exceeds the self-energy of an isolated dislocation of a given type (e.g., screw, edge, etc.) after a certain critical thickness. This approach was suggested for GeSi/Si heterostructures and gives the following expression for the critical thickness:

$$h_c \cong \left(\frac{1-\nu}{1+\nu}\right)\left(\frac{1}{16\pi\sqrt{2}}\right)\left[\frac{b^2}{a(x)}\right]\left[\left(\frac{1}{f^2}\right)\ln\left(\frac{h_c}{b}\right)\right]. \tag{4}$$

Van der Merwe[12] also calculated the critical layer thickness of a mismatched lattice overlayer on the basis of energy considerations. He considered the interfacial energy between the film and the substrate assuming a minimum energy available for generation of dislocations. The obtained critical thickness is, in its mathematical expression, very similar to that obtained by the geometrical model of Dunstan et al.[13] ($f = b/mh_c$, where m is a parameter fitted between 1 and 2),

$$h_c \cong \left(\frac{1-\nu}{1+\nu}\right)\left(\frac{1}{8\pi^2}\right)\frac{a_0}{f}. \tag{5}$$

Considering edge dislocations, i.e., the Burger vector b is equivalent to the diamond lattice parameter ($a_0 = 0.3566$ nm), and a Poisson parameter, ν, of 0.2 for diamond, the critical thickness corresponding to M–B, P–B, and V-M models can be deduced for the case of a

heavily boron-doped epilayer grown on an undoped diamond substrate. These three curves are graphed in Fig. 1 considering the respective diamond parameters.

As expected, the energy required to have a dislocation standing in the epilayer is very low for V-M and M–B approaches. The first one only considers interfacial energy, and the second one, bending existing dislocations; therefore, their deduced h_c is lower. However, in the case of a boron-doped diamond epilayer grown by MPCVD on a high-quality substrate, no dislocations are expected to be available in the substrate to begin the plastic relaxation (typical density below four dislocations/cm²).[17] Thus, the most appropriated model to diamond homoepitaxy for doped layers is that of P–B, where dislocation sources are activated when it is energetically favored. The blue area below the P–B curve indicates when thickness—[B] conditions are expected not to generate dislocations, i.e., predictions to grow dislocation-free layers. However, this region is limited by a blue line on its right-hand side. This line corresponds to the critical boron doping level (CBL)[14,15] that indicates the boron concentration limits above which dislocations are generated just at the growth surface. This occurs when two boron atoms are very close together on the growth surface. and thus, this criterion varies with the growth orientation.[18] This mechanism of dislocation generation is observed exclusively, until now, in diamond. It is induced by the strong atom diameter variations between carbon and dopant atoms as boron. As a general behavior, only a few atom types can be inserted into the diamond lattice and, apart from hydrogen, no atomic diffusion occurs in diamond. As a consequence, boron can be incorporated only during growth and the lattice strain induced, for a certain doping range, is close to those reached for III–V alloys, such as InGaAs/GaAs, or for SiGe/Si. Thus, when a boron atom takes its substitutional site in the diamond lattice, strong strain is generated around it and if another boron atom is also able to take another site close to the first one, dislocations can be generated in-between both atoms. This proximity effect mechanism, thus, strongly depends on (i) the growth conditions, i.e., facility for a boron atom to stand close to another one (for low growth rates and high temperatures, the atom can escape away from the proximity of the first one), and (ii) growth orientation as the atomic surface density change and in-plane strain also does. As shown in Table I, a critical boron concentration level (CBL) can be determined for the different growth orientations and CH₄/H₂ ratios.

In Fig. 1, the red dashed line indicates the CBL for a ⟨111⟩ growth orientation and a CH₄/H₂ ratio of 0.15%, while the blue one corresponds to the CBL for [100] growth orientation and a CH₄/H₂ ratio of

TABLE I. Critical boron concentration level (CBL) reported for different growing conditions.

Growth orientation	CH₄/H₂	CBL ($\times 10^{20}$ cm^{-3})	Comments
[100]	0.5	32	Sample #4
[100]	4	25	Ref. 15
[111]	0.15	17	Sample #1
[111]	0.6	6.5	Refs. 14 and 15
[111]	4	<10	Ref. 14
[111]	0.5	6.5	Sample #2
[111]	0.25	Unknown	Sample #3

0.5%. This proximity effect induces the generation of dislocations above an experimentally determined critical boron concentration.[15] Table I summarizes the CBL obtained for some different growth conditions.[19] These correspond to 2D mode growth conditions, which are not always the case during MPCVD growth as, for example, the Stranski–Krastanov one. A similar CBL is also observed during "lateral growth," i.e., growth on the lateral sides of terraces previously fabricated by inductively coupled plasma (ICP).[20] Such growth can also be assimilated to 2D growth as it takes place layer by layer and not by coalescence of pyramid-like structures. Most of the CBL values are shown to be close to some 10^{20} cm^{-3}. This indicates that this mechanism, in boron-doped diamond epilayers, is more frequent to that of uniform layer strain relaxation as described by P–B. Indeed, growth of more than 10 μm is necessary to reach h_c before the CBL (see the P–B curve). For example, using CH$_4$/H$_2$ = 4 on [100] orientation and [B] = 10^{21} cm^{-3} (i.e., below CBL, see Table I), a thickness above 10 μm is necessary to reach h_c (see Fig. 1, h_c for such doping and P–B curve), which is not a frequent value in MPCVD growth.

Another aspect that should be noticed is the type of dislocation generation through these "competitive" mechanisms: when dislocations are generated to relax the uniform lattice strain of an epilayer, they are generally pushed down to the substrate/epilayer interface by the Peach–Koehler force.[21–23] This is well reported in all the usual III–V systems such as InGaAs/GaAs[21,22] or SiGe/Si.[23] In contrast, the proximity effect mechanism considers that dislocations are generated at the growing plane only when two boron atoms are next to each other. Therefore, this is a random phenomenon that can occur at any location during the growth and no Peach–Koehler force is present in the epilayer to push the dislocation down to the substrate/epilayer interface, except if the M–B critical thickness is reached. In this case, strain is high enough to bend, i.e., also push, the dislocation down. As a result, in Fig. 2(a), dislocations are usually observed at any place in the epilayer. Black arrows in this figure indicate the location of dislocations that probably have been displaced by the Peach–Koehler force down in the epilayer depth, but those marked with white arrows are still at the top part of the epilayer. With a doping level of 2 × 10^{21} cm^{-3} and an epilayer thickness of 500 nm, this layer is located over the M–B critical thickness in the graph shown in Fig. 1. Thus, strain can bend dislocations, but below the critical thickness of P–B, which indicates that strain cannot activate dislocation sources. With a location below P–B h_c (see the red point in Fig. 1), above that of M–B and over its corresponding CBL (see Table I), sample #1 is just in an interesting range to analyze the dislocation behavior in heavily boron-doped diamond. P–B mechanisms cannot be activated, and thus, no dislocation resulting from strain relaxation can be present; but being above the CBL, proximity effects induce the presence of dislocations randomly in the epilayer depth. However, as observed in Fig. 2, considering the dislocations pointing out from the micrograph, i.e., dislocations lying in the growth plane (and not threading up as some others), their density is higher close to the substrate [see arrows B to E with respect to arrows in A in Fig. 2(a)]. This demonstrates that strain slightly pushes dislocations down even though it is not enough to push all of them down to the interface as usually observed in the P–B mechanism. Note that this sample #1 is out of its own dislocation-free region as its CBL is 10^{21} cm^{-3} (see Table I).

Comparing Figs. 1 and 2, it is found that layers located on the right-hand side of their CBL lines in Fig. 1 show the presence of
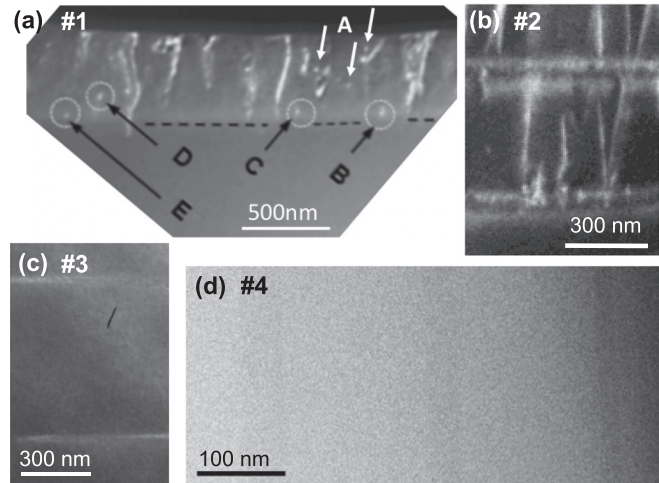

FIG. 2. (a) Dark field (DF) transmission electron microscopy (TEM) micrograph of sample #1 recorded in the $\langle 004 \rangle$ zone axis for sample #1. The growth orientation of the p++ 500-nm-thick epilayer is $\langle 111 \rangle$, with growth being performed using a CH$_4$/H$_2$ ratio of 0.15 and a doping level of 2 × 10^{21} cm^{-3}. Thus, its thickness stands below the P–B h_c (see the red point in Fig. 1). However, dislocations are observed. Their location is typical of the proximity generation mechanism, with all dislocations lying on the layer depth (see white points). (b) DF TEM micrograph of sample #2, growth along the [111] orientation, on the $\langle 001 \rangle$ zone axis recorded with the $[\bar{2}20]$ reflection, where the presence of dislocations is revealed in layer thicknesses around 20 nm (green point in Fig. 1). (c) DF TEM micrographs of sample #3 recorded in the $\langle 011 \rangle$ zone axis using the $[0\bar{2}2]$ reflection where no dislocations are observed. (d) High angle annular dark field (HAADF) TEM micrograph of sample #4 where three layers of 50, 20, and 10 nm are revealed without the presence of dislocations despite the very high doping level (2 × 10^{21} cm^{-3}). No defects are shown in these two last samples as their doping level is below their respective CBL (see the dashed green line in Fig. 1).

dislocations in Fig. 2. Even though the layer thickness is very small (some nanometers), proximity effects can generate dislocations as shown for sample #2 (green line). This behavior is shown to be strongly dependent on the growth orientation. Indeed, sample #4 has an identical CH$_4$/H$_2$ ratio but was grown along the $\langle 100 \rangle$ direction (in spite of $\langle 111 \rangle$); however, no dislocations are generated as it is placed on the left-hand side of its CBL line (in blue, Fig. 1). Sample #1, below the People and Bean h_c and above that of Mathews and Blakeslee in Fig. 1, has an interesting behavior. Despite the fact that it has a layer thickness below the People and Bean h_c, dislocations are generated as this sample is situated on the right-hand side with respect to its CBL line (red line, Fig. 1). As its thickness is above the Mathews and Blakeslee h_c, dislocations are shown to be pushed down to its lower interface (black arrows, Fig. 2). This behavior is not observed in sample #2 as it is located below the Mathews and Blakeslee h_c in the graph of Fig. 1.

In summary, conditions to grow dislocation-free boron-doped diamond epilayers on undoped substrates have been established and discussed. Key parameters, such as critical doping levels and epilayer thickness, have been quantified for the case of diamond boron doping, and the competitive strain relief and proximity effect mechanisms have been graphically compared. The resulting optimum growing conditions to reach heavily doped diamond layers without dislocation generation have been established.

DATA AVAILABILITY

The data that support the findings of this study are available from the corresponding author upon reasonable request.

REFERENCES

[1] N. Donato, N. Rouger, J. Pernot, G. Longobardi, and F. Udrea, J. Phys. D **53**, 093001 (2020).

[2] H. Umezawa, Mater. Sci. Semicond. Process. **78**, 147 (2018).

[3] E. Gheeraert, *Power Electronic Devices Applications of Diamond Semiconductors*, 1st ed. (Elsevier, Woodhead Publishing, Cambridge, 2018), Chap. 3.1, pp. 191–200.

[4] D. Prikhodko, S. Tarelkin, V. Bormashov, A. Golovanov, M. Kuznetsov, D. Teteruk, N. Kornilov, A. Volkov, and A. Buga, J. Superhard Mater. **41**, 24 (2019).

[5] S. Kono, T. Teraji, H. Kodama, and A. Sawabe, Diamond Relat. Mater. **63**, 30 (2016).

[6] C. Barbay, S. Saada, C. Mer-Calfati, S. Temgoua, J. Barjon, and J. C. Arnault, Appl. Surf. Sci. **495**, 143564 (2019).

[7] M. P. Gaukroger, P. M. Martineau, M. J. Crowder, I. Friel, S. D. Williams, and D. J. Twitchen, Diamond Relat. Mater. **17**, 262 (2008).

[8] R. Issaoui, A. Tallaire, A. Mrad, L. William, F. Bénédic, M. A. Pinault-Thaury, and J. Achard, Phys. Status Solidi A **216**, 1900581 (2019).

[9] D. Y. Liu, L. C. Hao, Z. A. Chen, W. K. Zhao, Y. Shen, Y. Bian, K. Tang, J. D. Je, S. M. Zhu, R. Zhang, Y. D. Zheng, and S. L. Gu, Appl. Phys. Lett. **117**, 022101 (2020).

[10] J. W. Matthews and A. E. Blakeslee, J. Cryst. Growth **27**, 118 (1974).

[11] R. People and J. C. Bean, Appl. Phys. Lett. **47**, 322 (1985).

[12] J. H. Van der Merwe, J. Appl. Phys. **34**, 123 (1963).

[13] J. D. Dunstan, S. Young, and R. H. Dixon, J. Appl. Phys. **70**, 3038 (1991).

[14] F. Lloret, D. Eon, E. Bustarret, A. Fiori, and D. Araujo, Nanomaterials **8**, 480 (2018).

[15] M. P. Alegre, D. Araujo, A. Fiori, J. C. Piñero, F. Lloret, M. P. Villar, P. Achatz, G. Chicot, E. Bustarret, and F. Jomard, Appl. Phys. Lett. **105**, 173103 (2014).

[16] V. V. Brazhkin, E. A. Ekimov, A. G. Lyapin, S. V. Popova, A. V. Rakhmanina, S. M. Stishov, and V. M. Levedev, Phys. Rev. B **74**, 140502(R) (2006).

[17] O. Loto, "Transistors en diamant pour électronique de puissance: études des matériaux et procédés technologiques," Ph.D. thesis (Communauté Université Grenoble Alpes, 2018).

[18] F. Lloret, D. Araujo, M. P. Alegre, J. M. Gonzalez-Leal, M. P. Villar, D. Eon, and E. Bustarret, Phys. Status Solidi A **212**, 2468 (2015).

[19] F. Lloret, D. Araujo, D. Eon, M. P. Villar, J. M. Gonzalez-Leal, and E. Bustarret, Phys. Status Solidi A **213**(10), 2570–2574 (2016).

[20] F. Lloret, A. Fiori, D. Araujo, D. Eon, M. P. Villar, and E. Bustarret, Appl. Phys. Lett. **108**, 181901 (2016).

[21] M. Gutiérrez, M. Herrera, D. González, G. Aragón, J. J. Sánchez, I. Izpura, M. Hopkinson, and R. García, Microelectron. J. **33**, 553 (2002).

[22] M. Gutiérrez, D. González, G. Aragón, R. García, M. Hopkinson, J. J. Sánchez, and I. Izpura, Appl. Phys. Lett. **80**, 1541 (2002).

[23] R. Gatti, F. Boioli, M. Grydlik, M. Brehm, H. Groiss, M. Glaser, F. Montalenti, T. Fromherz, F. Schäffler, and L. Miglio, Appl. Phys. Lett. **98**, 121908 (2011).